HHS Public Access

Author manuscript

Nano Lett. Author manuscript; available in PMC 2018 March 08.

Published in final edited form as:

Nano Lett. 2017 March 08; 17(3): 1356–1364. doi:10.1021/acs.nanolett.6b03815.

Tumor-penetrating nanosystem strongly suppresses breast tumor growth

Shweta Sharma[†], **Venkata Ramana Kotamraju**[†,‡], **Tarmo Mölder**[#], **Allan Tobi**[#], **Tambet Teesalu**[†,‡,#], and **Erkki Ruoslahti**[†,‡,*]

[†]Sanford-Burnham-Prebys Medical Discovery Institute, Cancer Research Center, La Jolla, CA, USA 92037

[‡]Center for Nanomedicine and the Department of Cell, Molecular and Developmental Biology, University of California, Santa Barbara, CA, USA 93106

[#]Laboratory of Cancer Biology, Institute of Biomedicine and Translational Medicine, University of Tartu, Tartu, Estonia 50411

Abstract

Antiangiogenic and vascular disrupting compounds have shown promise in cancer therapy, but tend to be only partially effective. We previously reported a potent theranostic nanosystem that was highly effective in glioblastoma and breast cancer mouse models, retarding tumor growth and producing some cures [Agemy et al. 2011,2013]. The nanosystem consists of iron oxide NPs ("nanoworms") coated with a composite peptide with tumor-homing and pro-apoptotic domains. The homing component targets tumor vessels by binding to p32/gC1qR at the surface or tumor endothelial cells. We sought to further improve the efficacy nanosystem by searching for an optimally effective homing peptide that would also incorporate a tumor-penetrating function. To this effect, we tested a panel of candidate p32 binding peptides with a sequence motif that conveys tumor-penetrating activity (CendR motif). We identified a peptide designated as Linear TT1 (Lin TT1) (sequence: AKRGARSTA) as most effective in causing tumor homing and penetration of the nanosystem. This peptide had the lowest affinity for p32 among the peptides tested. The low affinity may have moderated the avidity effect from the multivalent presentation on nanoparticles (NPs), such that the NPs avoid getting trapped by the so called "binding-site barrier", which can hinder tissue penetration of compounds with a high affinity for their receptors. Treatment of breast cancer mice with the LinTT1 nanosystem showed greatly improved efficacy compared to the original system. These results identify a promising treatment modality and underscore the value of tumor penetration effect in improving the efficacy tumor treatment.

[*]Correspondence to: Dr. Erkki Ruoslahti, Sanford-Burnham-Prebys Medical Discovery Institute, La Jolla, CA, 92037, USA; ruoslahti@sbpdiscovery.org.

Supporting Information Available: [The following methods are described in detail in SI Methods: Peptide homing to tumors and tumor treatment, immunohistochemistry, TUNEL staining, FA assay, cell cytotoxicity assay and immunoblot analysis.] This material is available free of charge via the Internet at http://pubs.acs.org.

Author contributions: SS, TT and ER conceived, designed the research. SS and ER wrote the manuscript. SS conducted the treatment and mechanistic studies. VRK synthesized the peptides and peptide conjugates.

Competing interests: ER and VRK are shareholders of EnduRx, a company that hold certain licensing rights on the LyP-1/TT1 technology.

Keywords

Cancer nanomedicine; Targeted drug delivery; Vascular disrupting agent; Tumor penetrating peptide; Iron-oxide nanoparticles; C-end Rule

Introduction

Drugs that block the growth of new blood vessels are a recent, important addition to the arsenal of oncologists.[1–4] Tumor vessels are different from normal vessels in terms of their morphology and biomarkers expression, and that makes it possible to target them for destruction with little effect on the vessels in normal tissues.[3]

We have previously described a NP-based vascular disrupting nanosystem consisting of a tumor-homing 5-amino acid peptide (CGKRK) fused to a pro-apoptotic peptide [$_D$(KLAKLAK)$_2$][5, 6] coupled to the surface elongated iron oxide NPs (nanoworms; NWs).[7] The CGKRK peptide is an effective tumor-homing peptide that binds to tumor endothelial cells and internalizes into them.[8, 9] When capable of accessing tumor cells, it also binds and enters into tumor cells of various types.

However, CGKRK does not extravasate and penetrate beyond tumor vessels, which makes the CGKRK-$_D$(KLAKLAK)$_2$-NWs a purely vascular disrupting agent. These NWs were highly effective when used to treat mice bearing glioblastomas; in one model, the growth of tumors was essentially completely suppressed, and in a more aggressive model, a substantial prolongation of the lifespan of the mice was achieved.[7] To provide extravasation and tumor-penetration functions, we co-administered the NWs with iRGD, which is a tumor-penetrating peptide capable of conferring such properties to compounds that are co-administered with the peptide, not coupled to it.[10–13] This nanosystem was significantly more effective in the aggressive glioblastoma model than the original NWs[7], presumably because the tumor cells had now also become a target. These results showed that having a vascular disrupting agent spread beyond the vasculature adds a valuable increment to the anti-cancer efficacy.

We subsequently identified the target molecule for the CGKRK peptide as cell surface p32 protein (also know as gC1qR and HABP), which is a mitochondrial protein expressed on the cell surface of activated (angiogenic) endothelial cells (and various kinds of tumor cells), but not in normal resting cells.[14,15] The identification of the receptor opened up a possibility of improving the original nanosystem by incorporating the tumor-homing function into the homing peptide. LyP-1 is cyclic 9-amino acid peptide that also uses p32 as its receptor (sequence: CGNKRTRGC).[16] Like CGKRK, LyP-1 internalizes into its target cells, but like iRGD, LyP-1 is also capable of penetrating into tumors and accumulates in the extravascular tumor tissue.[17,18] LyP-1 and iRGD contain a cryptic CendR (C-end Rule) motif (R/KXXR/K), which binds to neuropilin-1 (NRP-1) after the peptide has been cleaved by a cell surface protease.[10,19,20] The NRP-1 binding activates an endocytic pathway that transports payloads through the vascular wall and through tumor tissue, endowing these peptides with the tumor penetrating activity.[21] We have recently described the CendR peptide transport mechanism, new type of macropinocytosis that is receptor (NRP-1) dependent and nutrient

regulated. The uptake is linked to exocytosis and transfer to other cells.[22] CGKRK lacks the CendR function, and as a consequence, it mainly targets tumor blood vessels.

To provide the nanosystem an inherent tumor-penetrating capability, we tested a panel of peptides that recognize p32 and contain the CendR motif. Here we describe a new nanosystem that employs a low-affinity p32-binding peptide capable of rendering NPs highly effective in penetrating into cells and tumors, and in potentiating tumor treatment. Figure 1 schematically depicts the nanosystem and the current understanding of its mechanism of action.

Results

Tumor homing and penetration of p32-targeted NPs

We synthesized a panel of 9 different FAM-labeled p32-binding peptides for coupling to the NWs. The panel consisted of peptides with an existing CendR motif (LyP-1, and cyclic and linear TT1), as well as variations of the CGKRK peptide with an added CendR motif (Figure 2A). The peptides were covalently conjugated onto dextran coating of the NWs (Figure 2B). Fluorescence measurements showed that all peptides coupled at approximately the same efficiency, resulting in the coupling of approximately 22 nmol of peptide/mg of iron (Table S1).

TEM of the NWs after the amination step showed that iron oxide cores arranged into wormlike structures with an average length of 40-50 nm (Figure 2C; Table S1). Dynamic light scattering (DLS) measurements indicated an average size of 45nm (Table S1), which is in agreement with the TEM data and earlier reports.[7, 23–26] The average zeta potential (surface charge) of NWs after the amination step was strongly positive, 11.10mV (SD±0.36) in water (Table S1). Coupling of the 5K PEG linker to the NWs reduced the zeta potential to −1.35 mV, and the size increased by ~5 nm. PEG is known to impart a negative charge to NPs[23,36]. Further coupling of the peptide to the NWs through the linker did not substantially change the zeta potential or size (Figure 2D and E; Table S1).

We first tested NWs for their efficacy in homing and penetration into extravascular tumor tissue in MCF10CA1a breast tumors. NWs coated only with the homing peptide component were used in this experiment as a first indicator of treatment efficacy in the nanosystem context. A new CendR motif-containing p32-binding linear peptide, Linear TT1 (LinTT1; sequence: AKRGARSTA) was the most potent among the peptides in causing NWs accumulation in tumors, with much of the NW signal outside tumor blood vessels (Figure 3A). CGRKR(NH_2) (CGKRK with swapped lysines and arginines and amide-blocked C-terminus) and CGKRKRA (CGKRK with a cryptic CendR motif) were also more effective than CGKRK. The TT1 peptide was selected by screening a phage library expressing cyclic 9-amino acid peptides for peptides binding to recombinant p32 protein.[27] The cyclic TT1 peptide (CycTT1) binds p32 with a relatively high affinity (130 nM), higher than that of LyP-1 or CGKRK. However, on NPs, the low-affinity linear LinTT1 turned out to be the most effective peptide (Figure 3A). A summary of the quantified peptide-NW homing result is shown in Figure 3B. In addition to the tumors, NWs were detected in the liver and spleen, which non-specifically capture NPs regardless of their peptide coating. Other organs did not

contain significant numbers of NWs, confirming the specificity of the tumor homing (Figure S1). We noted that the cyclic TT1 peptide tended to cause aggregation of the peptide-coated NPs, which may contribute to the low activity of this peptide. Alternatively, the affinity/avidity of the NWs coated with CycTT1 or LyP-1 may have been so high that it caused a "binding-site barrier", which has been shown to prevent tissue spreading of other affinity ligands.[28]

Interaction of LinTT1 with p32 and NRP-1

The strong homing activity of the LinTT1-NWs was surprising because the LyP-1 peptide, when linearized has no detectable p32-binding activity. Thus, we expected the affinity of LinTT1 to be low or nondetectable. However, fluorescence anisotropy (polarization) assays revealed readily measurable affinity with a Kd of 8.7 μM for the LinTT1-p32 interaction, whereas the Kd of CycTT1 was 0.13 μM (Figure S2 A and B). When tested for binding to p32 and NRP-1, LinTT1 behaved as expected of a cryptic CendR peptide: the intact peptide bound to p32, but not to NRP-1, and the binding to the two proteins was reversed upon treatment of the peptide with the tumor-associated protease urokinase-type plasminogen activator (uPA) (Figure S3A). A control peptide with an active CendR motif, RPARPAR, bound only to NRP-1 regardless of uPA treatment (Figure S3B).

Tumor homing efficacy of homing peptide-$_D$(KLAKLAK)$_2$-NW conjugates

Based on the NW homing results, we selected LinTT1, CGKRKRA, and CGRKR(NH_2), for further study as $_D$[KLAKLAK]$_2$ conjugates on NWs. We also included CGKRK and LyP-1 for comparison. As shown previously, CGKRK-$_D$[KLAKLAK]$_2$-NWs accumulated in tumor blood vessels, without penetrating into extravascular tumor tissue.[7] LinTT1-$_D$[KLAKLAK]$_2$-NWs were highly effective in extravasating and penetrating tumor parenchyma (Figure 4A). The CGRKR(NH_2)-$_D$[KLAKLAK]$_2$-NWs and CGKRKRA-$_D$[KLAKLAK]$_2$-NWs also primarily localized with tumor blood vessels similar to LyP1, indicating that the intended CendR conversion was not effective, or that the activity of these peptides was not compatible with the $_D$[KLAKLAK]$_2$ peptide (Figure 4A). Quantification of the tumor accumulation showed that LinTT1-$_D$[KLAKLAK]$_2$-NWs are superior to other chimeric peptide-NWs; they were over 7-fold more effective than CGKRK-$_D$[KLAKLAK]$_2$-NWs (Figure 4B). In addition to non-specific accumulation of LinTT1-$_D$[KLAKLAK]$_2$-NWs in the liver and spleen, some fluorescence was seen in the kidney, presumably because label was on the non-degradable D-conformer form $_D$[KLAKLAK]$_2$ peptide, which is excreted into the urine (Figure S4). As has been shown for the LyP-1 peptide (Laakkonen et al., 2004; Fogal et al., 2008), LinTT1-NWs showed substantial overlap with tumor-associated macrophages/myeloid cells in tumor tissue (Figure S5).

We further tested the LinTT1-NWs and LinTT1$_D$[KLAKLAK]$_2$-NWs in two additional orthotopic breast tumor models: syngeneic tumors generated with 4T1 mouse breast cancer cells and MMTV-PyMT (transgenic breast cancer mice) tumors. Similar to what we observed in the MCF10Ca1A tumor model, both types of NWs efficiently homed to the vasculature of the 4T1 and MMTV-PyMT tumors, accumulating also in extravascular tumor tissue (Figure S6A and B). We also tested tumor accumulation and penetration of micelles as an alternative NP scaffold for LinTT1-$_D$(KLAKLAK)$_2$. Similar to the

LinTT1$_D$[KLAKLAK]$_2$-NWs, micelles prepared by self-assembly of lipid-tailed LinTT1-$_D$(KLAKLAK)$_2$ peptide strongly homed to tumor vasculature and also extravasated into tumor tissue in the MCF10CA1a tumor model (Figure S7). Thus tumor homing and accumulation caused by LinTT1-$_D$[KLAKLAK]$_2$ appears to be independent of the nature of the NP carrying the peptide.

Anti-tumor efficacy of NWs in breast tumor model

To investigate the therapeutic potential of LinTT1-$_D$[KLAKLAK]$_2$-NWs we tested these NWs in the MCF10CA1a breast cancer model. One of two independent experiments with similar results is shown in Figure 5A. The mean tumor volume of the PBS-treated group at three weeks was 830 mm^3. CGKRK-$_D$[KLAKLAK]$_2$-NWs and TT1-NWs, reduced the tumor volume about 50%, to 370 and 422 mm^3, respectively. LinTT1$_D$[KLAKLAK]$_2$-NWs were more effective with a mean tumor volume of 85 mm^3, representing about 90% reduction relative to the PBS control group and essentially no tumor growth (Figure 5B). In four out of 6 mice in the LinTT1$_D$[KLAKLAK]$_2$-NW group the tumor seemed to have disappeared. To see if the regressed tumors were eradicated, half of the mice with regressed tumors were observed for an additional 3 months and exhibited no tumor recurrence. LinTT1-NWs, with no $_D$[KLAKLAK]$_2$, also exhibited some anti-tumor activity similar to what has been shown for the LyP1 peptide.[17] These results show that LinTT1$_D$[KLAKLAK]$_2$-NWs are more effective than the previous NPs, and that the increased efficacy is likely due to a combination of the tumor-penetrating activity of LinTT1 and an inherent anti-tumor activity of TT1.

Histopathology of treated tumors

To gain insight to the mechanism of the anti-tumor activity of the LinTT1$_D$[KLAKLAK]$_2$-NWs, we performed histological analysis of the residual tumors at the end of the 3-week treatment period. The tumors showed extensive necrosis and a thin rim of tumor tissue around the necrotic core that contained many apparently apoptotic nuclei (Figure 5C).

Staining for the proliferation marker Ki67 showed intense staining with a high number of Ki67 positive nuclei (54%) in the PBS control tumors, including in the tumor rim (Figure 5D). The number of Ki67-positive cells in tumors treated with CGKRK$_D$[KLAKLAK]$_2$-NWs and LinTT1-NWs was reduced to 28% and 35%, respectively, while LinTT1$_D$[KLAKLAK]$_2$-NWs showed strongly reduced the Ki67 staining (7% positive nuclei in the tumor rim; Figure 5D). Thus, the enhanced antitumor effect of the LinTT1$_D$[KLAKLAK]$_2$-NWs appears to result from inhibition of cell proliferation and promotion of apoptosis in the tumors.

To determine the extent of vascularization in the treated tumors, we stained the tumor sections with the blood vessel marker CD31. The average blood vessels count in CGKRK$_D$[KLAKLAK]$_2$NWs treated sections were almost similar to LinTT1NW. LinTT1$_D$(KLAKLAK)$_2$NWs treated tumors showed marked reduction of blood vessels compare to PBS control which was more than 6 fold (Figure 5E).

To determine whether the accumulation of the LinTT1$_D$(KLAKLAK)$_2$-NWs in the tumors might decline as a result of the treatment, we tested NW homing to the residual treated

tumors at the end of treatment period. Tumors treated with LinTT1$_D$(KLAKLAK)$_2$-NWs showed no apparent decline in accumulation of TT1-NWs, with or without $_D$(KLAKLAK)$_2$ (Figure 6A; compare with Figure 4A). Approximately 68% of tumor vessels were positive for LinTT1$_D$(KLAKLAK)$_2$-NWs and 80% vessels were positive for LinTT1-NW. The homing of CGKRK$_D$[KLAKLAK]$_2$-NWs, which also bind to p32, to the treated tumors at 20% was also similar to their homing to untreated tumors (Figure 6B). Thus, the reason for the incomplete eradication of the tumors in some mice does not seem to be caused by the inability of the NWs to accumulate in the tumors.

TUNEL staining revealed the apoptosis in the LinTT1$_D$[KLAKLAK]$_2$-NW tumor rims, where it co-localized with the NWs (Figure 6C). The other NWs showed much less TUNEL staining, and the PBS control tumors were almost devoid of staining. In agreement with earlier results on the effects of the $_D$(KLAKLAK)$_2$ peptide on tumor cells, and on actively growing HUVECs, which resemble angiogenic endothelial cells[5], we found cell death accompanied by activation of caspase-3 in MCF10CA1a cultured tumor cells treated with LinTT1$_D$(KLAKLAK)$_2$-NWs (Figure S8). Finally, analyses of blood chemistry and tissue histology revealed no significant toxicity in the LinTT1$_D$(KLAKLAK)$_2$-NW-treated mice (Figure S9). These results define a tumor-penetrating nanosystem that is highly efficient in tumor treatment.

Discussion

We have designed anti-tumor nanosystem that incorporates a number of new features. It builds on a nanosystem previously shown to be highly effective in mouse models of glioblastomas and breast cancers[7,15], but uses a new tumor-targeting peptide. This peptide is more effective than the original CGKRK peptide in delivering the NPs to tumors, and confers the NPs tumor-penetrating properties as well as the ability to target tumor-associated macrophages in addition to tumor vessels and tumor cells. This tumor-penetrating function was provided for the original CGKRK-NWs by a separately injected tumor-penetrating peptide. As a result, the new system is simpler and more effective in tumor treatment than the original one.

The peptide we used for the new nanosystem was selected from among a number of peptides that recognize the same receptor as CGKRK, or were derived from CGKRK. The most effective peptide, LinTT1, was obtained by selecting from a phage library peptides capable of binding to recombinant p32 protein, and then converting the selected peptide to a linear form.[27] The superior tumor homing activity of the linear form of TT1, demonstrated in multiple tumor models, was surprising in that this peptide bound to p32 with a much lower affinity than the cyclic form and showed essentially no tumor-homing activity as a monomeric peptide. The likely reason for excellent activity profile of the linear peptide on NWs is the high avidity of the binding made possible by the multivalent presentation of the peptide.[29,30] At the same time, the low affinity of the free peptide may have prevented the avidity of the NPs for p32-displaying cell surfaces from becoming too high for optimal tissue penetration. It has been reported that high affinity of blood-brain barrier-targeting antibodies limits their release from receptors after transcytosis. This phenomenon is sometimes referred to as ‘binding-site or affinity barrier’, which denotes trapping of

antibodies where they first entered the target tissue. The result is unsatisfactory tissue spreading[32,33]. It may be that the relatively high affinity of peptides such as LyP-1 and cyclic TT1, combined with the avidity effect of NP presentation, elicits the affinity barrier effect. In contrast, TT1 may give the NPs an affinity that is more compatible with tissue penetration.

The LinTT1 result suggests that high affinity of a targeting ligand, which is critical in monovalent targeting, is not necessarily an advantage in the multivalent NP context. Remarkably, the presentation on NPs also greatly potentiates the activity of the drug peptide in the construct, the pro-apoptotic peptide, LinTT1$_D$(KLAKLAK)$_2$.[7,31] Thus, this nanosystem vividly illustrates some of the advantages of nanotechnology in drug delivery.

The LinTT1-NWs showed excellent homing and penetrating activity in several breast cancer models, including the MCF10CA1A model used in a treatment study. Moreover, the homing was specific for tumors; as no fluorescence was found in normal tissues not known to non-specifically capture all NPs (liver and spleen) or secrete NP degradation products (kidney). The lack of detectable toxicity, even in the liver, which takes up NPs, was another indication of the specificity of the nanosystem.

The LinTT1-based nanosystem was significantly more effective in tumor treatment than the original system, which itself was more effective than many other treatments tested.[7] A significant proportion (10/14) the tumors regressed as a result of the treatment with LinTT1$_D$(KLAKLAK)$_2$-NWs, and the mice in this group that were followed up remained tumor-free for several months. The efficacy of the system is likely to result from the superior homing properties of the LinTT1-coated NWs, but other factors may contribute. LyP-1, the prototype p32-binding homing peptide possesses an inherent anti-tumor effect. LyP-1 alone, without any drug, causes apoptosis in the cells that take up the peptide most avidly, tumor macrophages in particular, causing elimination of these cells from the tumor.[14,17] LinTT1 peptide may have similar activity.

The NP nature of our anti-cancer agent raises the question as to whether the peptide acts as a NW conjugate or is released from the NWs. We have previously demonstrated that p32-binding NPs show co-localization with mitochondria after cellular uptake.[7] We have also shown that that NP-coupled $_D$[KLAKLAK]$_2$ is hundreds of times more active than free $_D$[KLAKLAK]$_2$.[7] The $_D$[KLAKLAK]$_2$ dose we used was adjusted accordingly and is so low that free homing peptide-$_D$[KLAKLAK]$_2$ conjugate would have no activity. Based on these considerations, we conclude that the active form of the nanosystem is likely the intact particle. The low dose of the NP form also makes it possible to essentially eliminate the considerable toxicity of free homing peptide $_D$[KLAKLAK]$_2$ conjugates. Thus it is essential that the chimeric peptide be presented on an NP. However, the system is adaptable, in that the nature of the NP scaffold does not seem to be important because micelle-based particles were also effective.

The efficacy and relative simplicity of the nanosystem based on a single chimeric peptide coupled to the surface of NWs, which are not unlike iron oxide NPs approved for clinical use in anemia treatment and as a MRI contrast agent, augur well for potential clinical utility of the system. Moreover, the iron oxide NP scaffold is potentially theranostic. Finally, the

drug peptide is mechanistically different from the standard chemotherapy drugs, and may be effective against tumors resistant to other treatments, although that remains to be shown. An effort is underway to complete pre-clinical studies necessary for the advancement of this system to clinical trials.

Methods

Peptide synthesis and NW conjugates

Peptides were synthesized with a 5(6)-fluorescein carboxylate (FAM) label, and an extra cysteine with a free sulfhydryl group was added to cyclic peptides as described (Kotamraju et al. 2016). The synthesis and subsequent conjugation of aminated dextran coated iron oxide nanoworms (NWs) have been described.[7,23–26] For peptide coupling to NWs, aminated NWs were PEGylated with maleimide-5KPEG-NHS (JenKem Technology) and peptides were conjugated to the functionalized particles through a thioether bond between the cysteine thiol in the peptide and the maleimide on the particles. Transmission electron microscopy (TEM) imaging to visualize the NWs was conducted using a Philips CM100 electron microscope. NW size was determined on NanoSight instrument (Malvern Instruments Ltd., Malvern, UK) using a 1mg/mL solution of particles in sterile double distilled water.

Cell lines and tumors

The MCF10CA1a human breast tumor cell line was obtained from the Barbara Ann Karmanos Cancer Institute (Detroit, MI). Cells were maintained in Dulbecco's Modified Eagle Medium (DMEM) supplemented with 10% fetal bovine serum, 1% Glutamine-Pen-Strep and 100 ng/ml (Sigma-Aldrich, St. Louis, MI). The 4T1 murine breast cancer cells were purchased from the American Type Culture Collection (Manassas, VA). The cells were maintained in DMEM supplemented with 10% fetal bovine serum and 1% Glutamine-Pen-Strep at 37°C/5% CO_2. Human umbilical vein endothelial cells (HUVEC; Lonza Walkersville, Walkersville, MD) were cultured using EBM-2 medium with endothelial cell growth supplement (Lonza).

To produce MCF10CA1a tumors, BALB/c nude mice were orthotopically injected into the mammary fat pad with 2×10^6 cells suspended in 100 μl of PBS. The 4T1 cells (1×10^6) were implanted subcutaneously in the flanks of 4-week-old BALB/c mice. FVB-Tg(c3-1-TAg)Cjeg/JegJ mice (Jackson Laboratory, Bar Harbor, Maine), which develop spontaneous breast cancers, were maintained in the animal facility at Sanford-Burnham-Prebys Medical Discovery Institute. Animal experimentation was performed according to procedures approved by the Sanford-Burnham-Prebys IACUC.

Supplementary Material

Refer to Web version on PubMed Central for supplementary material.

Acknowledgments

This work was supported by grants R01CA188883 (ER), and Cancer Center Support grant CA30199 to Sanford Burnham Prebys from the National Cancer Institute of NIH, and grant R44 CA183287 to EnduRx Pharmaceuticals.

TT was supported by Susan Komen for Cure Foundation Award KG110704, European Research Council Starting Grant GliomaDDS from European Regional Development Fund, and Wellcome Trust International Fellowship (WT095077MA).

References

1. Ferrara N, Alitalo K. Nat Med. 1996; 5:1359–1364.
2. Hanahan D, Folkman J. Cell. 1996; 86:353–364. [PubMed: 8756718]
3. Ruoslahti E, Bhatia SN, Sailor SJ. J Cell Biol. 2010; 188:759–768. [PubMed: 20231381]
4. Pham E, Yin M, Peters CG, Lee CR, Brown D, Xu P, Man S, Jayaraman L, Rohde E, Chow A, Lazarus D, Eliasof S, Foster FS, Kerbel RS. Cancer Res. 2016; 76:4493–503. [PubMed: 27325647]
5. Ellerby HM, Arap W, Ellerby LM, Jain R, Andrusiak R, Rio GD, Krajewski S, Lombardo CR, Rao R, Ruoslahti E, Bredesen DE, Pasqualini R. Nat Med. 1999; 9:1032–1038.
6. Arap W, Haedicke W, Bernasconi M, Kain R, Rajotte D, Krajewski S, Ellerby HM, Bredesen DE, Pasqualini R, Ruoslahti E. Proc Natl Acad Sci USA. 2002; 99:1527–1531. [PubMed: 11830668]
7. Agemy L, Friedmann-Morvinski D, Kotamraju VR, Roth L, Sugahara KN, Girard OM, Mattrey RF, Verma IM, Ruoslahti E. Proc Natl Acad Sci U S A. 2011; 108:17450–17455. [PubMed: 21969599]
8. Joyce JA, Laakkonen P, Bernasconi M, Bergers G, Ruoslahti E, Hanahan D. Cancer Cell. 2003; 4:393–403. [PubMed: 14667506]
9. Hu Q, Gao X, Kang T, Feng X, Jiang D, Tu Y, Song Q, Yao L, Jiang X, Chen H, Chen J. Biomaterials. 2013; 34:9496–9508. [PubMed: 24054848]
10. Sugahara KN, Teesalu T, Karmali PP, Kotamraju VR, Agemy L, Girard OM, Hanahan D, Mattrey RF, Ruoslahti E. Cancer Cell. 2009; 16:510–520. [PubMed: 19962669]
11. Akashi Y, Oda T, Ohara Y, Miyamoto R, Kurokawa T, Hashimoto S, Enomoto T, Yamada K, Satake M, Ohkohchi N. Br J Cancer. 2014; 110:1481–1487. [PubMed: 24556620]
12. Wang K, Zhang X, Liu Y, Liu C, Jiang B, Jiang Y. Biomaterials. 2014; 35:8735–8747. [PubMed: 25023394]
13. Ni D, Ding H, Liu S, Yue H, Bao Y, Wang Z, Su Z, Wei W, Ma G. Small. 2015; 11:2518–2526. [PubMed: 25678130]
14. Fogal V, Zhang L, Krajewski S, Ruoslahti E. Cancer Res. 2008; 68:7210–7218. [PubMed: 18757437]
15. Agemy L, Friedmann-Morvinski D, Kotamraju VR, Sharma S, Sugahara KN, Ruoslahti E. Molecular Therapy, 2013. 21:2195–2204.
16. Laakkonen P, Porkka K, Hoffman JA, Ruoslahti E. Nat Med. 2002; 8:751–755. [PubMed: 12053175]
17. Laakkonen P, Akerman ME, Biliran H, Yang M, Ferrer F, Karpanen T, Hoffman RM, Ruoslahti E. Proc Natl Acad Sci USA. 2004; 101:9381–6938. [PubMed: 15197262]
18. Roth L, Agemy L, Kotamraju VR, Braun G, Teesalu T, Sugahara KN, Hamzahand J, Ruoslahti E. Oncogene. 2012; 31:3754–3763. [PubMed: 22179825]
19. Teesalu T, Sugahara KN, Kotamraju VR, Ruoslahti E. Proc Natl Acad Sci USA. 2009; 106:16157–16162. [PubMed: 19805273]
20. Sugahara KN, Teesalu T, Karmali PP, Kotamraju VR, Agemy L, Greenwald DR, Ruoslahti E. Science. 2010; 328:1031–1035. [PubMed: 20378772]
21. Kadonosono T, Yamano A, Goto T, Tsubaki T, Niibori M, Kuchimaru T, Kizaka-Kondoh S. J Control Release. 2015; 10:14–21.
22. Pang HB, Braun GB, Friman T, Aza-Blanc P, Ruidiaz ME, Sugahara KN, Teesalu T, Ruoslahti E. Nat Comm. 2014; 5:1–12.
23. Park J-H, Von Maltzahn G, Zhang L, Schwartz MP, Bhatia SN, Ruoslahti E, Sailor MJ. Adv Mater. 2008; 20:1630–1635. [PubMed: 21687830]
24. Park J-H, Von Maltzahn G, Zhang L, Derfus AM, Simberg D, Harris TJ, Bhatia SN, Ruoslahti E, Sailor MJ. Small. 2009; 5:694–700. [PubMed: 19263431]
25. Simberg D, Duza T, Park JH, Essler M, Pilch J, Zhang L, Derfus AM, Yang M, Hoffman RM, Bhatia S, Sailor MJ, Ruoslahti E. Proc Natl Acad Sci U S A. 2007; 16:932–936.

26. Agemy L, Sugahara KN, Kotamraju VR, Gujraty K, Girard OM, Kono Y, Mattrey RF, Park JH, Sailor MJ, Jimenez AI, Cativiela C, Zanuy D, Sayago FJ, Aleman C, Nussinov R, Ruoslahti E. Blood. 2010; 14:2847–2856.
27. Paasonen LS, Sharma S, Braun G, Kotamraju VR, Chung T, She ZG, Sugahara KN, Yliperttula M, Wu B, Pellecchia M, Ruoslahti E, Teesalu T. Chembiochem. 2016; 17:570–575. [PubMed: 26895508]
28. Fujimori K, Covell DG, Fletcher JE, Weinstein JN. J Nucl Med. 1990; 7:1191–1198.
29. Reulen SW, Dankers PY, Bomans PH, Meijer EW, Merkx M. J Am Chem Soc. 2009; 131:7304–7312. [PubMed: 19469576]
30. Ruoslahti E. Adv Mater. 2012; 24:3747–3756. [PubMed: 22550056]
31. Standley SM, Toft DJ, Cheng H, Soukasene S, Chen J, Raja SM, Band V, Band H, Cryns VL, Stupp SI. Cancer Res. 2010; 70:3020–3026. [PubMed: 20354185]
32. Fujimori K, Covell DG, Fletcher JE, Weinstein JN. J Nucl Med. 1990; 31:1191–8. [PubMed: 2362198]
33. Moos T, Morgan EH. J Neurochem. 2001; 79(1):119–29. [PubMed: 11595764]
34. Karmali PP, Kotamraju VR, Kastantin M, Black M, Missirlis D, Tirrell M, Ruoslahti E. Nanomedicine. 2009; 5(1):73–82. [PubMed: 18829396]
35. She ZG, Liu X, Kotamraju VR, Ruoslahti E. ACS Nano. 2014; 28(10):10139–49.
36. Nazli C, Ergenc TI, Yar Y, Acar HY, Kizilel S. Int J Nanomedicine. 2012; 7:1903–1920. [PubMed: 22619531]

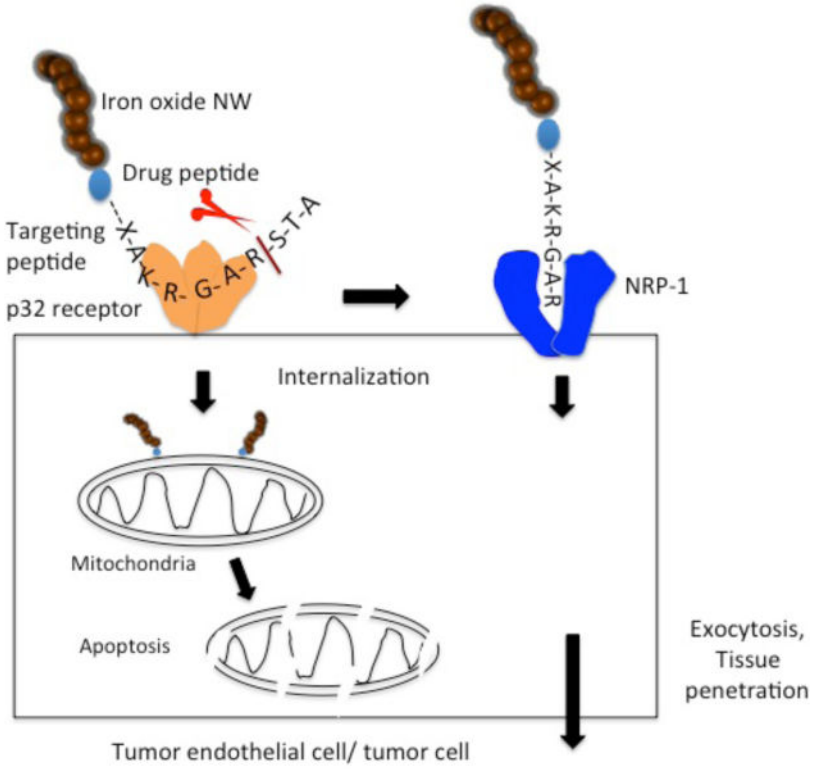

Figure 1. Schematic representation of the nanosystem and current understanding of its mechanism of action

The system is built on an elongated iron oxide NP (nanoworm; NW) scaffold, with multiple copies of a tandem peptide comprised of a homing peptide and a pro-apoptotic/cytotoxic peptide conjugated onto the surface of the NW. The tumor-homing peptide has two activities: the intact peptide binds to cell surface p32 on tumor vessel endothelium (and on tumor cells and tumor associated macrophages). The peptide is internalized into cells expressing cell surface p32 and transported to mitochondria. A truncated form of the peptide, created by proteolysis at the cell surface, subsequently binds to neuropilin-1 (NRP-1) through its CendR (R/KXXR/K) motif, which triggers a macropinocytosis-related transcytosis and trans-tissue transport pathway (CendR pathway). The NWs are swept into this pathway and out of the vasculature and into extravascular tumor tissue. The pro-apoptotic peptide serves the anti-cancer drug in the construct (see ref.30 for references).

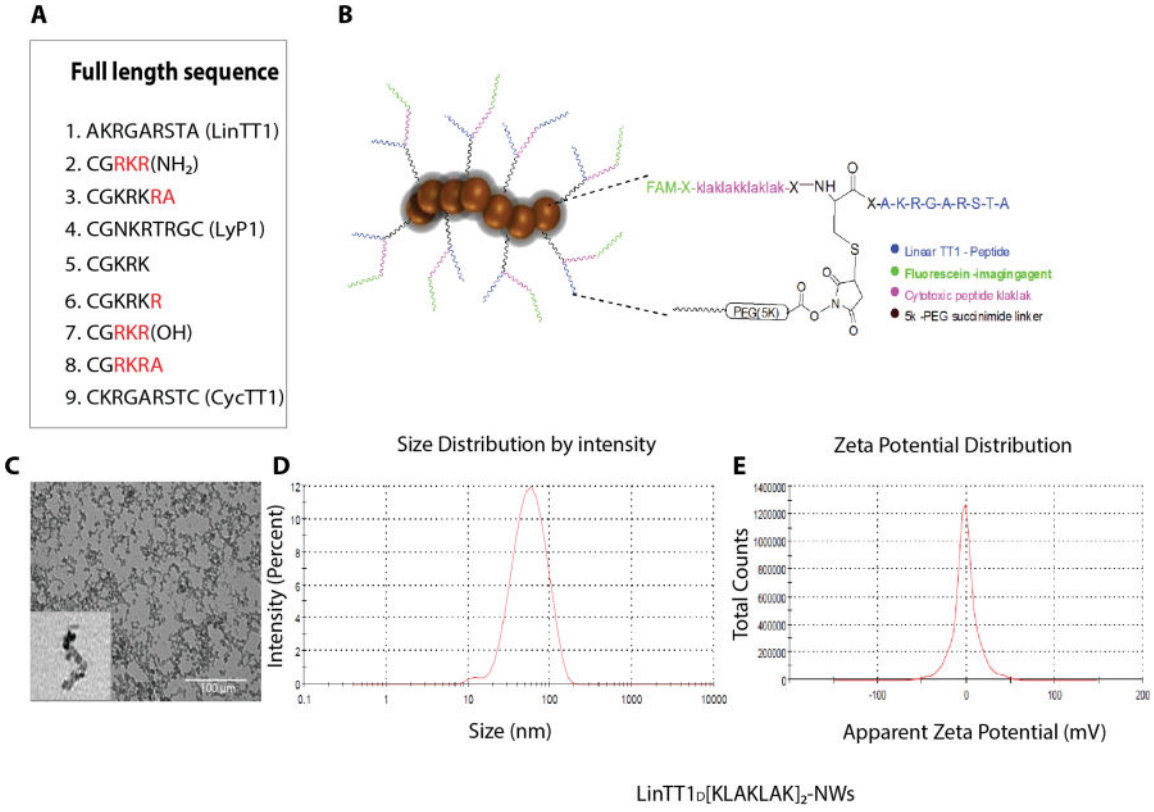

Figure 2. Design of tumor-homing peptides and NWs

(A) A total of nine p32-binding-peptides were synthesized to test *in vivo* tumor homing. (B) A chimeric peptide combining a tumor-homing peptide (LinTT1 in this example) with a pro-apoptotic peptide is covalently coupled to NWs; length 40-50 nm). An extra cysteine was added to the N-terminus of the LinTT1 peptide and used for coupling to NWs. The drug peptide and the FAM fluorophore were attached to the free N-terminus of the cysteine residue. (C) Transmission Electron Microscopy (TEM) image of NWs after the amination step. (D) Size of LinTT1-$_D$[KLAKLAK]$_2$ conjugated NWs as determined by dynamic light scattering (DLS). (E) Zeta potential of LinTT1-$_D$[KLAKLAK]$_2$-NWs as measured by DLS.

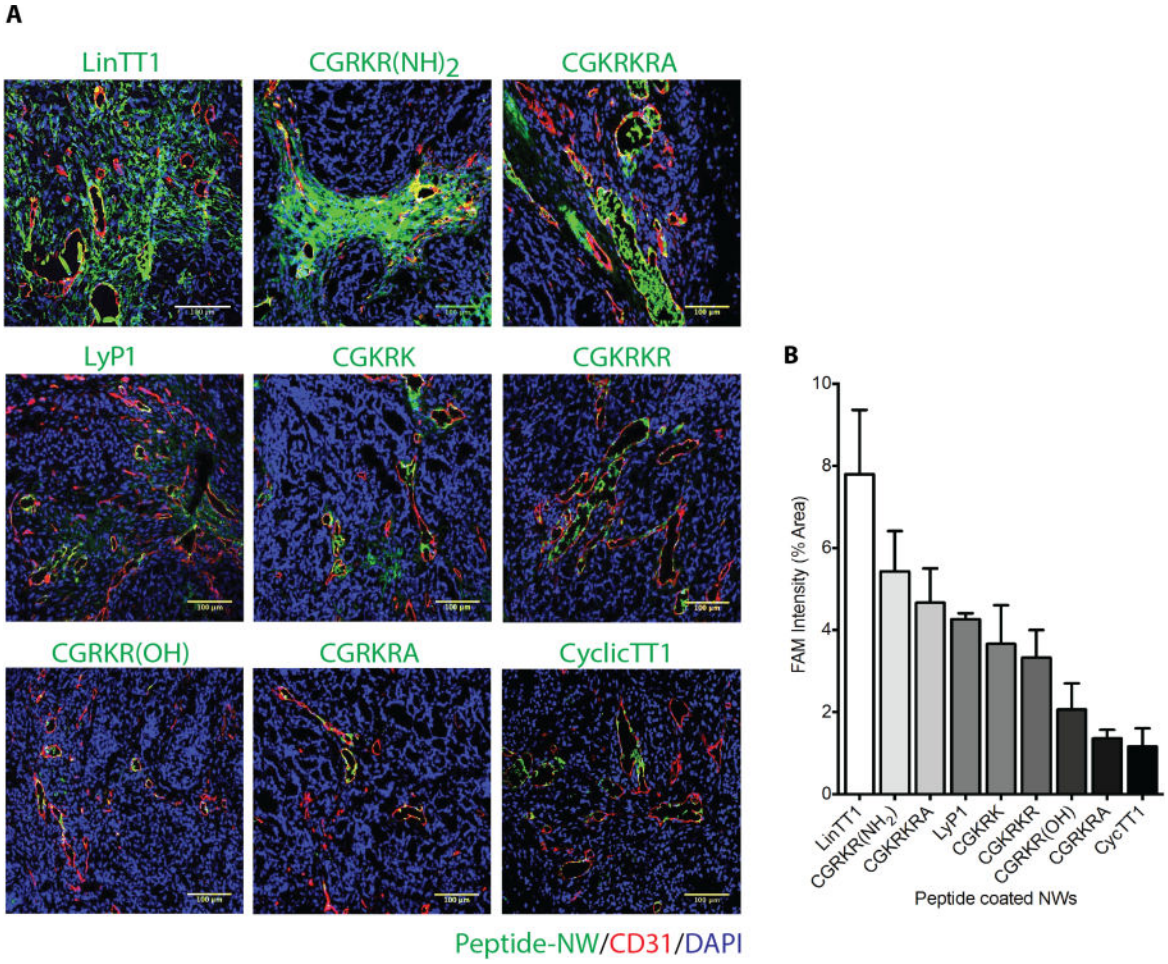

Figure 3. Tumor homing of TT1-NWs

(A) Mice bearing orthotopic MCF10CA1a breast cancer xenografts were intravenously injected with peptide-coated-NWs (7.5mg iron/kg), and the NWs were allowed to circulate for 5 hours. The mice were perfused through the heart with PBS, and tumors and organs were collected and processed for fluorescence microscopy. A representative confocal microscopy image for each peptide from tumors in 3 mice is shown. Merged image: green, NWs, red, CD31; blue, nuclei. Scale bars 100μm. Striking accumulation of FAM-LinTT1-NWs outside tumor blood vessels is seen. (B) Quantification of tumor accumulation of NWs. Slides were scanned using Scanscope. Ten random areas in each tumor section (n = 3/group) were selected for quantification of NW fluorescence using ImageJ software. Error bars = mean ±SD.

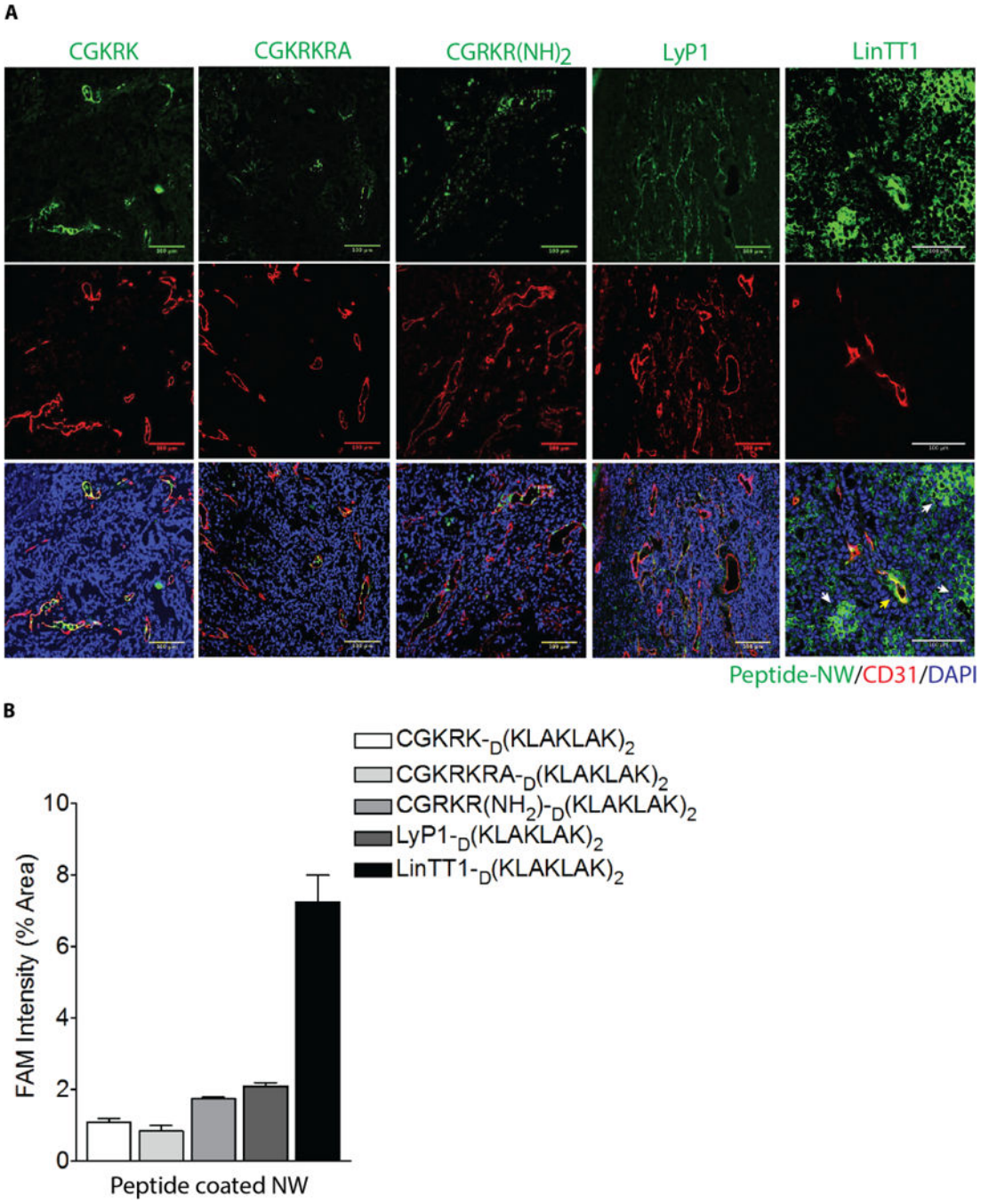

Figure 4. Tumor homing of NWs coated with chimeric peptides consisting of a homing peptide and pro-apototic peptide

(A) Representative confocal images showing NW homing to MCF10CA1a tumors. LinTT1-$_D$[KLAKLAK]$_2$-NWs partially co-localize with tumor blood vessels (CD31), but most of the NWs are outside the blood vessels in the extravascular tumor tissue. (B) Quantification of NW fluorescence in tumors.

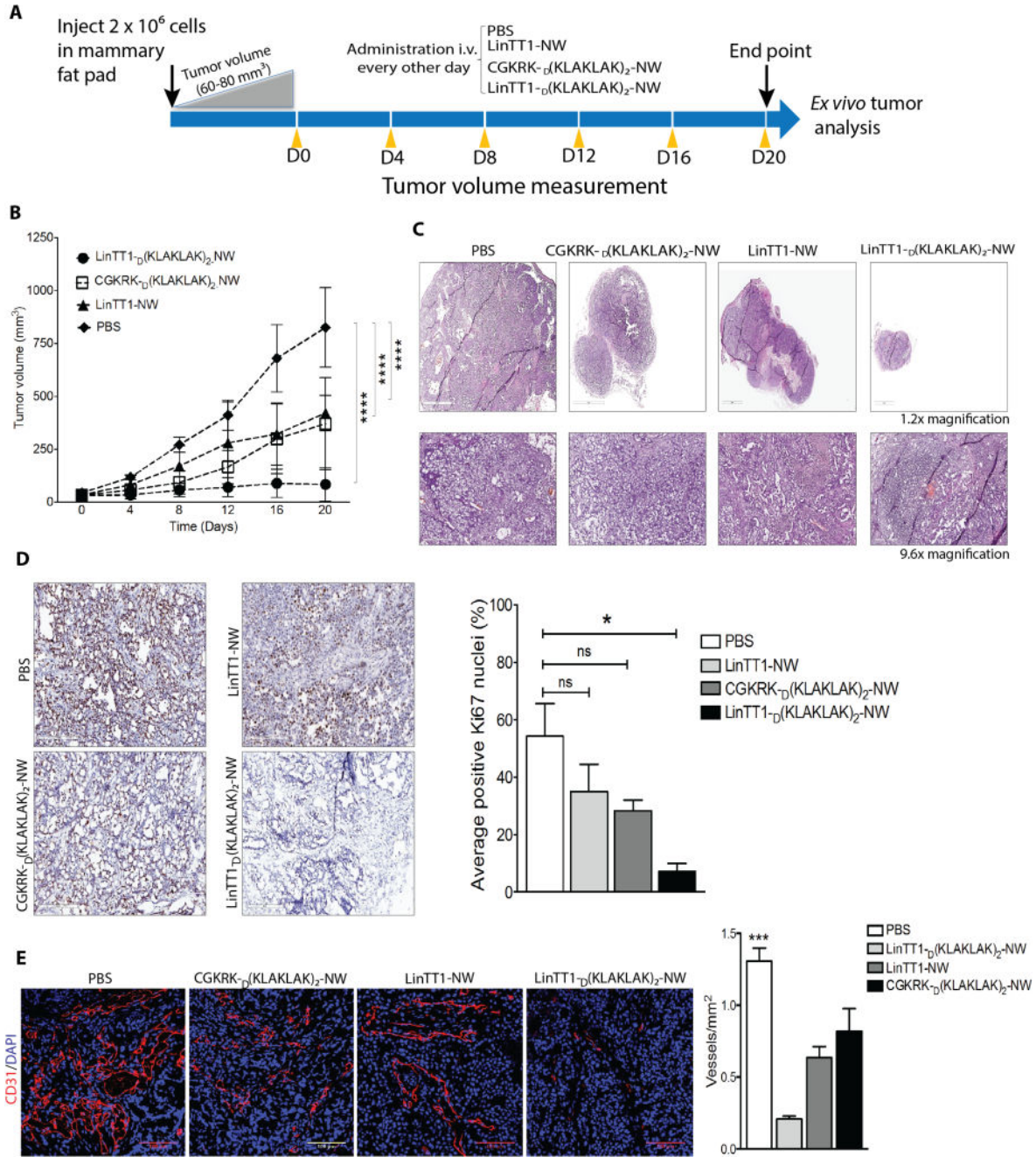

Figure 5. Therapeutic efficacy of LinTT1-$_D$[KLAKLAK]$_2$-NWs in MCF10CA1a tumor mice

(A) Schematic representation of treatment approach. (B) Mice bearing MCF10CA1a orthotopic tumor xenografts were intravenously injected with peptide-coated NWs every other day for 3 weeks at a dose of 7.5mg of iron/kg (similar to the daily dose of iron used in anemia treatment). PBS, n = 5; LinTT1-NW, n = 5; CGKRK$_D$[KLAKLAK]$_2$-NWs, n = 6; LinTT1$_D$[KLAKLAK]$_2$-NWs, n = 6. One of two independent experiments with similar results is shown. Error bars, mean ± SD. Statistical analyses were performed with ANOVA; ****P < 0.0001. (C) Representative sections stained with hematoxylin and eosin (H&E). (D) Sections from treated tumors were stained with an antibody specific for proliferating cell

nuclear antigen (Ki67). The graph shows percentage of Ki67 positive nuclei. The results are expressed as a mean ±SD (*$P < 0.01$, one way ANOVA, Kruskal-Wallis test $n = 3$ mice per group). Scale bar = 200μm. (E) Representative confocal images tumor vasculature stained with anti-CD31 (red). Blood vessels were quantified by counting 10 random fields at 20× magnification, and the results are presented as number of vessels per field (***$P < 0.001$, one way ANOVA, Tukey's posthoc test, $n = 3$ mice per group) S cale bar = 100μm).

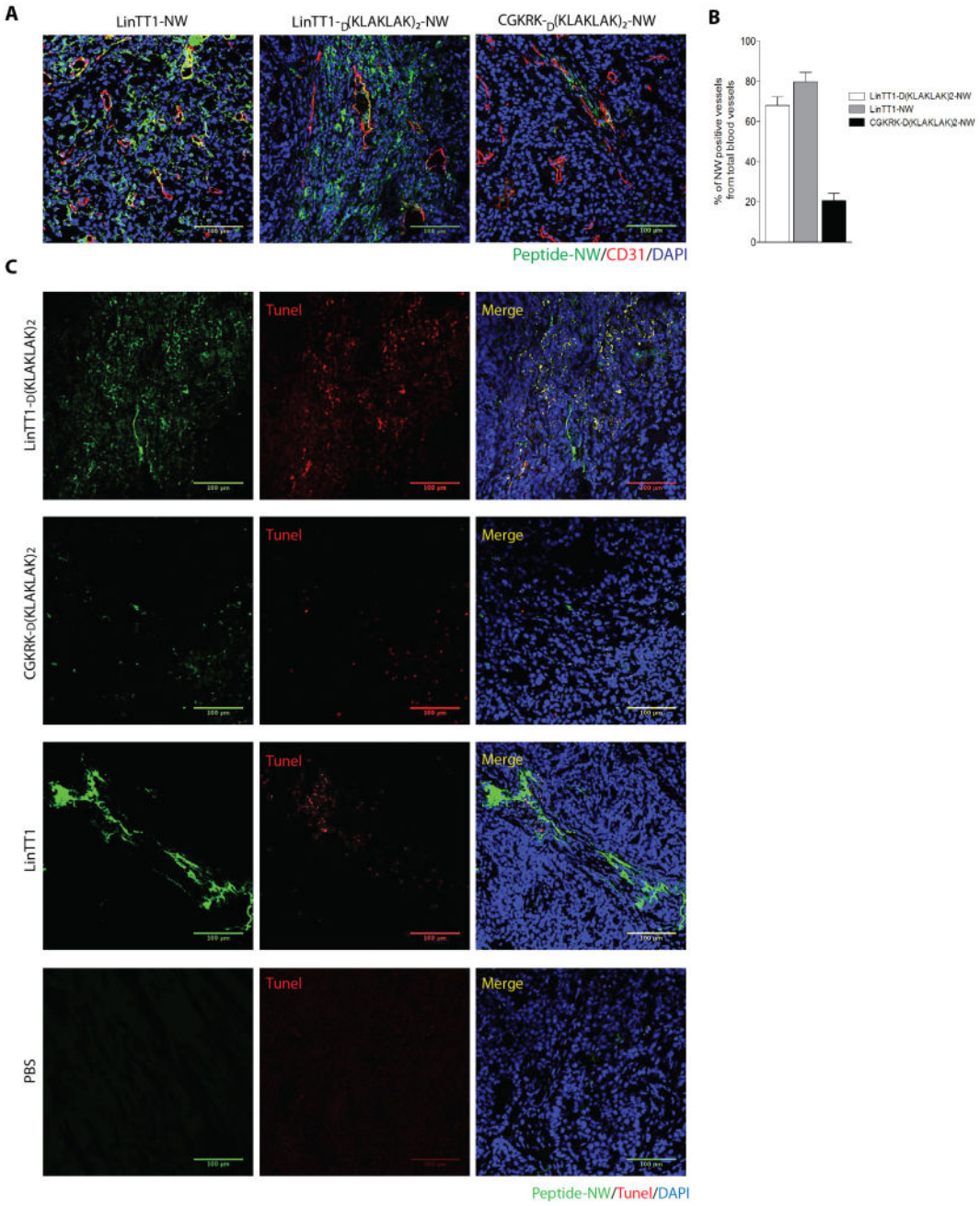

Figure 6. Accumulation of peptide-coated NWs and apoptosis in blood vessels of treated tumors

(A) Confocal images showing tumor accumulation of FAM-labeled peptide-NWs after three weeks of treatment. Five hours after the last injection, the mice were perfused through the heart with PBS, and tissues were collected. Tumor sections were stained with anti-CD31 and examined by confocal microscopy. Green, NWs; red, blood vessels; blue, DAPI-stained nuclei. (Scale bars, 100μm.) (B) Quantification of peptide-NWs. Percentage of NW-positive blood vessels was determined in confocal microscopy by analyzing 10 random areas in each tumor section (n = 3/group). Error bars = mean ±SD, scale bar = 100μm. (C) TUNEL staining of treated tumors after three weeks of treatment with the indicated NWs. Merged

image: green, NWs; red, TUNEL-positive nuclei; blue, nuclei stained with DAPI. Scale bars, 100μm.